

Calculation of the transport and relaxation properties of methane. II. Thermal conductivity, thermomagnetic effects, volume viscosity, and nuclear-spin relaxation

Robert Hellmann,¹ Eckard Bich,² Eckhard Vogel,¹ Alan S. Dickinson,^{2,a)} and Velisa Vesovic³

¹*Institut für Chemie, Universität Rostock, D-18059 Rostock, Germany*

²*School of Chemistry, Newcastle University, Newcastle upon Tyne NE1 7RU, United Kingdom*

³*Department of Earth Science and Engineering, Imperial College London, London SW7 2AZ, United Kingdom*

(Received 14 January 2009; accepted 20 February 2009; published online 25 March 2009)

Transport properties of pure methane have been calculated in the rigid-rotor approximation using the recently proposed intermolecular potential energy hypersurface [R. Hellmann *et al.*, *J. Chem. Phys.* **128**, 214303 (2008)] and the classical-trajectory method. Results are reported in the dilute-gas limit for the temperature range of 80–1500 K. The calculated thermal conductivity values are in very good agreement with the measured data and correlations. In the temperature range of 310–480 K the calculated values underestimate the best experimental data by 0.5%–1.0%. We suggest that the calculated values are more accurate, especially at low and high temperatures, than the currently available correlations based on the experimental data. Our results also agree well with measurements of thermal transpiration and of the thermomagnetic coefficients. We have shown that although the dominant contribution to the thermomagnetic coefficients comes from the \mathbf{W}_{jj} polarization in the spherical approximation, the contribution of a second polarization, \mathbf{W}_j , cannot be neglected nor can a full description of the \mathbf{W}_{jj} polarization. The majority of the volume viscosity measurements around room temperature are consistent with the calculated values but this is not the case at high and low temperatures. However, for nuclear-spin relaxation the calculated values consistently exceed the measurements, which are mutually consistent within a few percent. © 2009 American Institute of Physics. [DOI: 10.1063/1.3098317]

I. INTRODUCTION

The accurate calculation of the transport and relaxation properties of simple molecular gases directly from the intermolecular potential energy hypersurface has recently become possible.^{1–8} These calculations provide not only a stringent test of the accuracy of the potential surface but also an accurate data set at low and high temperatures, where experimental data are more difficult to measure and hence are of lower accuracy or nonexistent. For methane, which is relevant to a wide variety of topical issues including climate change and energy sustainability and may even have been observed⁹ on an exoplanet, the provision of accurate transport and relaxation properties is important since this reduces the uncertainty in modeling processes where methane properties play a major role.

In the first paper of this series,¹⁰ to be referred to as I, results of classical-trajectory calculations for the shear viscosity, viscomagnetic effects, and self-diffusion of pure methane have been reported. In the present paper we report on calculations for thermal conductivity, thermomagnetic coefficients, volume viscosity, and nuclear-spin relaxation. As methane has an isotropic polarizability, no depolarized Rayleigh light scattering measurements, available for other mol-

ecules studied,^{1,4,8} are possible. Thus this work completes the evaluation of transport and relaxation properties of methane. The calculations of these properties are based on formal kinetic theory, which provides a unified description of transport and relaxation phenomena in terms of generalized cross sections.¹¹ The relevant cross sections have been evaluated by means of classical-trajectory calculations directly from the recent *ab initio* potential.¹² This potential has been adjusted to and validated against accurate experimental second pressure virial coefficient data and subsequently its reliability confirmed using accurate viscosity data.¹⁰

The intermolecular potential employed was developed using the zero-point vibrationally averaged configuration, which limited the collision dynamics to treating methane molecules as rigid rotors. Although it was shown¹⁰ that results using the rigid-rotor assumption are consistent with experiment for the viscosity and self-diffusion coefficients of methane at temperatures up to 1050 K, for thermal conductivity the neglect of energy transport by vibrationally excited molecules becomes more questionable. In order to estimate the influence on the thermal conductivity of neglecting vibration we have employed the approximation described in our previous work.^{5–8} Hence we have corrected, where necessary, the generalized cross sections obtained from the classical-trajectory calculations based on the rigid-rotor assumption. For carbon dioxide the approximate procedure for

^{a)}Electronic mail: a.s.dickinson@newcastle.ac.uk. Author to whom correspondence should be addressed.

the inclusion of the effects of the vibrational degrees of freedom has been shown⁷ to lead to good agreement with the available experimental data on the thermal conductivity and the thermomagnetic effect.

The transport and relaxation properties are reported in the temperature range of 80–1500 K. It is not *a priori* clear that the classical-trajectory method will retain its accuracy at low temperatures. Comparison with the quantum calculations for the He–N₂ system^{13,14} indicates that the accuracy of the classical-trajectory calculations deteriorates rapidly with decreasing temperature. However, as there exist data for thermal conductivity and thermomagnetic effects somewhat below 100 K, these data can be used to estimate the accuracy of classical-trajectory calculations at such temperatures.

In Sec. II we summarize the basic theory employed and the results are discussed in Sec. III. A summary and conclusions are presented in Sec. IV.

II. THEORY

A. Thermal conductivity

The thermal conductivity λ of a polyatomic gas at zero density and in the absence of external fields can be expressed as¹¹

$$\lambda = \frac{5k_B^2 T}{2m\langle v \rangle_0} \frac{\mathfrak{S}(1001) - 2r\mathfrak{S}\left(\begin{smallmatrix} 1001 \\ 1010 \end{smallmatrix}\right) + r^2\mathfrak{S}(1010)}{\mathfrak{S}(1010)\mathfrak{S}(1001) - \mathfrak{S}\left(\begin{smallmatrix} 1001 \\ 1010 \end{smallmatrix}\right)^2} f_\lambda^{(n)}, \quad (1)$$

where $\langle v \rangle_0 = 4(k_B T / \pi m)^{1/2}$ is the average relative thermal speed, m is the molecular mass, T is the temperature, and k_B is Boltzmann's constant. The quantities $\mathfrak{S}(1010)$, $\mathfrak{S}(1001)$, and $\mathfrak{S}\left(\begin{smallmatrix} 1001 \\ 1010 \end{smallmatrix}\right)$ are generalized cross sections, and the notation and conventions employed are fully described elsewhere.^{10,11}

The parameter r is given by

$$r = \left(\frac{2 c_{\text{int}}}{5 k_B} \right)^{1/2}, \quad c_{\text{int}} = c_{\text{rot}} + c_{\text{vib}}. \quad (2)$$

Here c_{int} is the contribution of both the rotational, c_{rot} , and the vibrational, c_{vib} , degrees of freedom to the isochoric heat capacity c_V .

The quantity $f_\lambda^{(n)}$ is the n th-order correction factor for the thermal conductivity and accounts for the effects of higher basis-function terms in the perturbation-series expansion of the solution of the Boltzmann equation.¹¹ Only the second-order correction factor has been derived for thermal conductivity, but it includes contributions from both velocity coupling^{11,15} and angular-momentum coupling.^{11,16,17} In second order the velocity coupling involves the inclusion of all the members of the usual basis set¹¹ Φ^{10sr} with $s+t \leq 2$. The resulting expressions¹⁸ for thermal conductivity involve 15 generalized cross sections. The contribution due to angular momentum is dominated by the polarization $\mathbf{W}_{\mathbf{j}\mathbf{j}}$ and requires the inclusion of the tensorial basis function $\Phi^{1200|1}$ in the expansion. The expressions for the thermal conductivity have been given by Viehland *et al.*¹⁷ and more recently, in an equivalent but simpler form by Bich *et al.*⁵ Our previous

calculations^{2,3,5,7} indicate that both contributions are small, of the order of $+(1-2)\%$, and numerous calculations based on spherical potentials¹⁹ confirm this for the velocity-coupling contribution. Hence the combined second-order contribution, $f_\lambda^{(2)}$, can be estimated by adding the two contributions. In total, a knowledge of 18 generalized cross sections is required to calculate the overall second-order contribution using the expressions given by Maitland *et al.*,¹⁸ Viehland *et al.*,¹⁷ or Bich *et al.*⁵

Traditionally the solution of Boltzmann's equation has been sought by using the basis functions that belong to the two-flux basis set and results in the expression given by Eq. (1).¹¹ For thermal conductivity this amounts to treating the transport of translational and internal energy separately. Thijsse *et al.*,²⁰ by using the same basis functions but choosing different scalars, constructed an equivalent total-energy basis set. In the first approximation in this basis the thermal conductivity, λ^{10E} , is governed by only one generalized cross section,

$$\lambda^{10E} = \frac{5k_B^2 T}{2m\langle v \rangle_0} \frac{1+r^2}{\mathfrak{S}(10E)}. \quad (3)$$

This new cross section, $\mathfrak{S}(10E)$, is a linear combination of the three cross sections used to describe the thermal conductivity in the two-flux approach,^{7,11,20}

$$\mathfrak{S}(10E) = \frac{1}{1+r^2} \left[\mathfrak{S}(1010) + 2r\mathfrak{S}\left(\begin{smallmatrix} 1010 \\ 1001 \end{smallmatrix}\right) + r^2\mathfrak{S}(1001) \right]. \quad (4)$$

For subsequent analysis of the experimental data on the closely related process of thermal transpiration we give here the expression for the dimensionless translational Eucken factor f_{tr} in terms of the relevant cross sections,

$$f_{\text{tr}} \equiv \frac{2m\lambda_{\text{tr}}}{3k_B\eta} \approx \frac{5}{3} \frac{\mathfrak{S}(2000) \left[\mathfrak{S}(1001) - r\mathfrak{S}\left(\begin{smallmatrix} 1001 \\ 1010 \end{smallmatrix}\right) \right] f_{\lambda_{\text{tr}}}^{(2)}}{\mathfrak{S}(1010)\mathfrak{S}(1001) - \mathfrak{S}\left(\begin{smallmatrix} 1001 \\ 1010 \end{smallmatrix}\right)^2} f_\eta^{(3)}. \quad (5)$$

Here λ_{tr} is the contribution of the translational degrees of freedom to the thermal conductivity and η denotes the shear viscosity coefficient. The first terms of Eq. (5) define f_{tr} and the final term relates this to generalized cross sections and higher-order correction factors.

B. Thermomagnetic effects

It is well documented¹¹ that in the presence of a magnetic (or electric) field the coupling between the velocity and angular momentum is partially destroyed and the thermal conductivity coefficient loses its isotropic character. Three independent thermal conductivity coefficients are necessary to describe fully the resulting behavior.

When the magnetic field is oriented perpendicular to the temperature gradient two thermomagnetic coefficients measure the change in thermal conductivity in the perpendicular,

$\Delta\lambda^\perp$, and transverse, λ^{tr} , directions. The remaining thermomagnetic coefficient $\Delta\lambda^\parallel$ measures the change in thermal conductivity when the field is oriented parallel to the temperature gradient.¹¹

For linear and spherical-top molecules there is overwhelming experimental evidence that the dominant polarization needed in the solution of Boltzmann's equation is $\mathbf{W}\mathbf{j}\mathbf{j}$.¹¹ However, this evidence is based on the analysis of the experimental data by means of a spherical approximation (SA), which simplifies the working equations.¹¹ It is unclear at present if small deviations of the experimental data from the theory are due to the use of the SA or to the neglect of other polarizations. The current work will allow us to investigate both possibilities and test the validity of the experimental analyses based solely on the $\mathbf{W}\mathbf{j}\mathbf{j}$ polarization.

The general expressions for the thermal conductivity in a magnetic field due to a single $\mathbf{W}\mathbf{j}\mathbf{j}$ polarization were first derived by Tip.²¹ For conciseness we give here an expression for the transverse thermomagnetic coefficient only using an alternative notation:²²

$$\frac{\lambda^{\text{tr}}}{\lambda} = -\frac{\Psi_{12}}{2}\{5K_1\xi_{12} + [10Y(2Z - K_1) - 2K_2K_3Z]\xi_{12}^3\} \times [1 + (9Z^2 - 4Y)\xi_{12}^2 + 4Y^2\xi_{12}^4]^{-1}. \quad (6)$$

Similar expressions for the other two coefficients and the definitions of the quantities K_L , Y , and Z are given in Ref. 7. The dimensionless field parameter ξ_{pq} is given by¹¹

$$\xi_{pq} = \frac{g_{\text{rot}}\mu_N k_B T}{\hbar \langle v \rangle_0} \frac{1}{\mathfrak{S}(pq00)_0} \frac{B}{P}. \quad (7)$$

Here g_{rot} is the rotational g factor, μ_N is the nuclear magneton, B is the magnitude of the magnetic flux density, and P is the pressure.

The quantity Ψ_{pq} in Eq. (6), which governs the magnitude of the contribution for a given pq polarization, is given by¹¹

$$\begin{aligned} \Psi_{pq} = & \frac{3}{5} \left\{ \overline{\mathfrak{S}} \begin{pmatrix} 1010 \\ pq00 \end{pmatrix} \left[r \mathfrak{S} \begin{pmatrix} 1010 \\ 1001 \end{pmatrix} - \mathfrak{S}(1001) \right] \right. \\ & \left. + \overline{\mathfrak{S}} \begin{pmatrix} 1001 \\ pq00 \end{pmatrix} \left[\mathfrak{S} \begin{pmatrix} 1010 \\ 1001 \end{pmatrix} - r \mathfrak{S}(1010) \right] \right\}^2 \\ & \times \left\{ \overline{\mathfrak{S}}(pq00)^{(1)} \left[\mathfrak{S}(1010)\mathfrak{S}(1001) - \mathfrak{S} \begin{pmatrix} 1010 \\ 1001 \end{pmatrix}^2 \right] \right. \\ & \left. \times \left[\mathfrak{S}(1001) - 2r \mathfrak{S} \begin{pmatrix} 1010 \\ 1001 \end{pmatrix} + r^2 \mathfrak{S}(1010) \right] \right\}^{-1}. \end{aligned} \quad (8)$$

In the SA, in which the collision operator acts separately on the directions of the velocities and of the angular momenta, it is assumed that $\overline{\mathfrak{S}}(1200)^{(1)} = \overline{\mathfrak{S}}(1200)^{(0)}$ and $K_1 = K_2 = K_3 = Y = Z = 1$. Equation (6) then reduces to the well-known, simple, expression¹¹

$$\frac{\lambda^{\text{tr}}}{\lambda} = -\frac{1}{2}\Psi_{12}^{\text{SA}}[g(\xi_{12}) + 2g(2\xi_{12})], \quad (9)$$

where $g(x) = x/(1+x^2)$.

As far as we are aware, no general expressions have been derived for thermomagnetic effects that include polarizations other than $\mathbf{W}\mathbf{j}\mathbf{j}$. Hence, the influence of other polarizations can only be examined within the spherical-approximation framework. Inclusion of the $\mathbf{W}\mathbf{j}$ polarization leads to the following expression for the transverse thermomagnetic coefficient:

$$\frac{\lambda^{\text{tr}}}{\lambda} = -\frac{1}{2}\Psi_{12}^{\text{SA}}[g(\xi_{12}) + 2g(2\xi_{12})] + \Psi_{11}^{\text{SA}}g(\xi_{11}). \quad (10)$$

Similar expressions for the other two ratios are given in p. 346 of Ref. 11.

The present calculations provide us with all the cross sections necessary to calculate the quantities Ψ_{pq} , K_L , Y , Z , and the parameter ξ_{pq} , required for the evaluation of the three thermomagnetic coefficients. Hence we are in a position to ascertain what influence, if any, inclusion of the second polarization, Eq. (10), and/or the full treatment, Eq. (6), has on the thermomagnetic coefficients obtained by the traditional approach, Eq. (9).

C. Volume viscosity

The volume viscosity (also known as the bulk viscosity) can be inferred from measurements of the absorption and dispersion of ultrasonic waves in the gas.¹¹ As noted by Prangma *et al.*,²³ for the analysis of sound-absorption measurements the volume viscosity η_V is the fundamental quantity of interest. In this work we limit our investigation to the contribution to volume viscosity that arises from rotational relaxation only, as the nature of the intermolecular potential used in the calculation precludes investigation of the vibrational relaxation process.

The volume viscosity can be written as

$$[\eta_V]_n = \frac{k_{BC\text{int}}}{c_V^2} \frac{k_B T}{\langle v \rangle_0 \mathfrak{S}(0001)} f_{\eta_V}^{(n)}. \quad (11)$$

The quantity $f_{\eta_V}^{(n)}$ is the n th-order correction factor for the volume viscosity and accounts for the effects of higher basis-function terms in the perturbation-series expansion of the solution of the Boltzmann equation.¹¹ The explicit expression for the second-order kinetic theory expression, $[\eta_V]_2$, is given by Maitland *et al.*¹⁸ We have also investigated employing a third-order expression, $[\eta_V]_3$, obtained as for the second-order result¹⁸ but by using a basis set¹¹ Φ^{00st} with $s+t \leq 3$. (See also the discussion in I¹⁰ of the analogous higher-order expressions for the shear viscosity.)

A number of experimenters have presented their measurements of sound absorption and dispersion in terms of a relaxation time τ_{expt} . Because the volume viscosity, rather than the relaxation time, is the fundamental quantity measured, also because it is for the volume viscosity that higher-order kinetic theory is available, we have converted these relaxation time measurements to volume viscosity values using the first-order kinetic theory relation¹¹

$$[\eta_V]_1 = \frac{k_{BC\text{int}} P \tau_{VT}}{c_V^2},$$

$$[\eta_V]_n \approx \frac{k_B c_{\text{int}} P \tau_{\text{expt}}}{c_V^2}, \quad (12)$$

where τ_{VT} is the isothermal relaxation time.^{23,24} Use of this equation to convert measured relaxation times to volume viscosity values is only approximately equivalent to analyzing the measurements in terms of the volume viscosity.

D. Nuclear-spin relaxation

Due to the alignment of the nuclear magnetic moments when a static magnetic field is present, a weak equilibrium magnetization occurs in a polyatomic gas. A nonequilibrium nuclear magnetization can then be caused by absorption of radio-frequency radiation and the nuclear-spin system will return to equilibrium. Johnson and Waugh²⁵ and Bloom *et al.*²⁶ concluded that spin rotation is the dominant relaxation mechanism in gaseous methane. Oosting and Trappeniers²⁷ showed that this mechanism is responsible for 90% or more of the relaxation. Jameson *et al.*²⁸ estimated that, for methane, mechanisms other than spin-rotation relaxation give relaxation rates orders of magnitude smaller than spin rotation. In principle two relaxation times are present for $^{12}\text{CH}_4$ molecules^{11,29} but, in practice, all measurements have been analyzed using just one. Furthermore, the measurements appear consistent, within experimental error, with a single relaxation time.^{26,28,29} In this case the cross section governing the relaxation¹¹ is $\mathfrak{S}'(0100)$, where the prime indicates that the contribution from just one of the collision partners is included. For a fuller discussion see Ref. 8.

III. RESULTS

The classical-trajectory calculations were performed using an extension of the TRAJECT software code for linear molecules,³⁰ modified³¹ to allow for the additional variables and averaging needed for asymmetric tops. The methane molecule was represented as a rigid spherical top and the interaction of two methane molecules is described by a six-dimensional *ab initio* intermolecular potential energy hypersurface.¹² All the details of the classical-trajectory calculations and the intermolecular potential are summarized in I.¹⁰

The calculated transport and relaxation cross sections¹¹ relevant to the present paper are characterized by the customary monotonic decrease with temperature, while some of the production cross sections¹¹ exhibit a maximum at low temperature. The values of the transport and relaxation cross sections are, on average, an order of magnitude larger than those of the production cross sections. Based on the convergence tests, the precision of most of the calculated transport and relaxation cross sections is estimated to be better than $\pm 0.1\%$, while the precision of most of the production cross sections is estimated to be better than $\pm 1.0\%$, at all except the very lowest temperatures.

Tables of all the relevant generalized cross sections resulting directly from the classical-trajectory computations and of the thermal conductivity coefficients calculated in this work have been deposited with the Electronic Physics Auxiliary Publication Service.³²

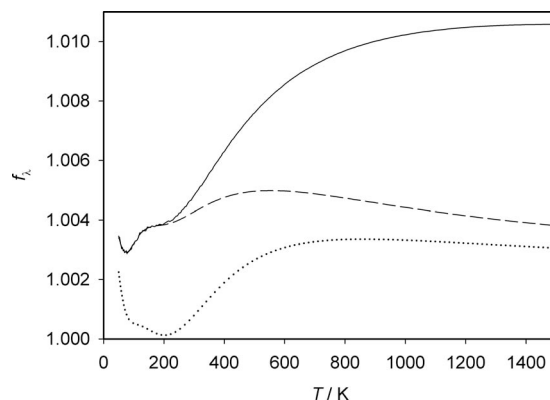


FIG. 1. Comparison of the values of the two second-order corrections $f_{\lambda}^{(2)}$ (---), $f_{\lambda}^{(2')}$ (.....), and of the rigid-rotor correction $f_{\lambda,rr00}^{(2)}$ (—) for the thermal conductivity coefficient.

A. Thermal conductivity

1. Vibrational degrees of freedom

To account for the vibrational degrees of freedom we have corrected, using the methodology and notation described in Ref. 7, all the cross sections $\mathfrak{S}_{p'q's't'}^{pqst}$ with $t+t' > 0$ which enter the description of thermal conductivity both in the absence and presence of the field. In the first-order approximation for thermal conductivity, $n=1$ in Eq. (1), two such cross sections are present. The vibrational correction for $\mathfrak{S}(1001)_{rr00}$ is small and weakly dependent on temperature and the resulting $\mathfrak{S}(1001)_{\text{int}}$ is at most 6% lower than $\mathfrak{S}(1001)_{rr00}$ at 600 K. Here the subscripts “rr00” and “int” denote values calculated with and without the vibrational correction, respectively. The vibrational correction for the production cross section $\mathfrak{S}_{1001}^{(1010)}_{\text{int}}$ is larger and exhibits a strong temperature dependence, as already noted for CO_2 . At 1500 K the ratio $\mathfrak{S}_{1001}^{(1010)}_{\text{int}}/\mathfrak{S}_{1001}^{(1010)}_{rr00}$ is 0.43. However, at high temperatures the production cross section is approximately 30 times smaller than the two transport cross sections; hence its contribution to the thermal conductivity is small. The overall effect on the thermal conductivity of correcting the cross sections for the vibrational degrees of freedom is almost negligible, of the order of 0.06% at 600 K, increasing in magnitude to 0.24% at 1500 K. For comparison the correction at 600 K for CO_2 , with its low-lying vibrational level, amounted to 5%. Hence, we are confident that the present calculations, based on the rigid-rotor intermolecular potential, are accurate up to the quoted high-temperature limit of 1500 K.

2. Second-order contributions

The overall, second-order thermal conductivity correction factor $f_{\lambda}^{(2)}$ has been calculated as described in Ref. 7 using the expressions given by Maitland *et al.*¹⁸ and Bich *et al.*⁵ All the relevant cross sections of the type $\mathfrak{S}_{10s't'}^{10st}$ with $t+t' \neq 0$ that enter these expressions have been corrected for the influence of the vibrational degrees of freedom using the methodology described in Ref. 7.

Figure 1 illustrates the temperature dependence of the overall second-order thermal conductivity correction factor $f_{\lambda}^{(2)}$. The magnitude of the correction is small, reaching a

maximum value of 0.5% at approximately 550 K. As expected, the correction is smaller than that observed for carbon dioxide.

In order to ascertain the influence of the vibrational degrees of freedom we have also calculated the overall second-order correction factor using the rigid-rotor values for the cross sections and have labeled the resulting correction $f_{\lambda,rr00}^{(2)}$. As illustrated in Fig. 1, $f_{\lambda,rr00}^{(2)}$ increases with temperature, reaching the value of 1.01 at high temperature. Although the vibrational degrees of freedom exert an increasing influence with increasing temperature, their influence on the magnitude of the overall second-order correction factor is such that the thermal conductivity would change by less than 0.7%.

Figure 1 also illustrates the temperature dependence of the second-order thermal conductivity correction factor $f_{\lambda}^{(2')}$ due to the velocity polarization alone. Above temperatures of about 200 K the magnitude of this correction factor increases with temperature, reaching a maximum value of approximately 1.003. By comparing the values of $f_{\lambda}^{(2)}$ and $f_{\lambda}^{(2')}$ it can be seen that the angular-momentum coupling contribution is also small, exhibiting a maximum value of 1.0035 at 220 K but then rapidly decreasing with increasing temperature.

Similarly to viscosity, the angular-momentum coupling contribution is smaller for methane than for any of the other three gases studied, especially at temperatures above room temperature, consistent with the production cross sections, $|\mathcal{S}_{10st}^{(1200)}|$, being smaller for methane.

3. Use of the total-energy basis set

The values of thermal conductivity have been also calculated by means of the Thijssse approximation, Eq. (3). The agreement with the calculations based on the first-order, two-flux, approach [Eq. (1) with $f_{\lambda}^{(n)}=1$], is excellent, to better than $\pm 0.5\%$ over the whole temperature range. This confirms the finding that for all the molecules studied so far^{2,3,7} the Thijssse approximation gives very good estimates of the first-order thermal conductivity. It also provides further evidence that a single cross section, $\mathcal{S}(10E)$, is sufficient to describe closely the behavior of the thermal conductivity.

4. Translational Eucken factor

For a number of gases Millat *et al.*³³ performed a series of thermal transpiration experiments that allow the determination of the translational Eucken factor f_{tr} [see Eq. (5)] and consequently evaluation of the contribution of the translational degrees of freedom to the thermal conductivity. For methane, the thermal transpiration experiments were performed in the temperature range of 300–600 K. The primary pressure-temperature data obtained in the experiments were analyzed by means of the integrated-dusty-gas model to obtain the values of the translational Eucken factor. These values were subsequently fitted to a suitable temperature function and the authors estimated the uncertainty of their results as $\pm 1\%$.

Values of f_{tr} were calculated using Eq. (5). The agreement with the values inferred from the thermal transpiration

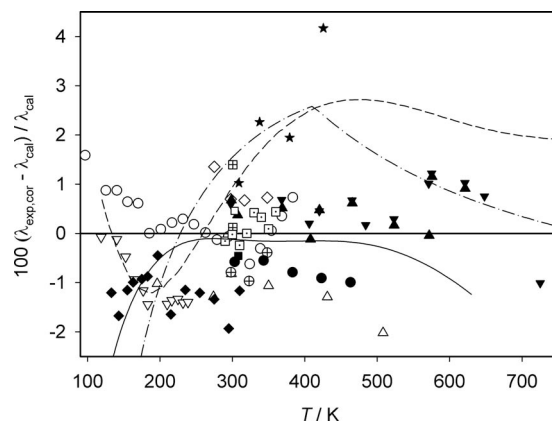


FIG. 2. Deviations of experimental and correlated zero-density thermal conductivity coefficients from values calculated for CH_4 . Experimental data: (○) Johnston and Grilly (Ref. 39); (△) Golubev (Ref. 40); (◇) Mistic and Thodos (Ref. 41); (▽) Sokolova and Golubev (Ref. 42); (▲) Le Neindre *et al.* (Ref. 43); (▼) Tufeu *et al.* (Ref. 44); (□) Clifford *et al.* (Ref. 45); (⊕) Tanaka *et al.* (Ref. 46); (⊞) Clifford *et al.* (Ref. 47); (■) Assael and Wakeham (Ref. 48); (◆) Roder (Ref. 49); (●) Hemminger (Ref. 50); (★) Millat *et al.* (Ref. 51); (◻) Pátek and Klomfar (Ref. 52). Correlations: (—) Friend *et al.* (Refs. 34 and 35); (---) Assael *et al.* (Ref. 36); (-·-·-) Uribe *et al.* (Refs. 37 and 38).

measurements³³ is excellent with deviations decreasing monotonically with increasing temperature from +1.2% at 300 K to -0.1% at 600 K.

5. Comparison with experiment

Around 1990 several correlations were performed for the thermal conductivity of methane in the limit of zero density.^{34–38} These correlations not only were based on a critical evaluation of thermal conductivity measurements but also employed theoretical considerations, especially when extrapolating to high temperatures.

In Fig. 2 the correlations and selected experimental data^{39–52} are compared with the calculations of the present paper. The hot-wire (HW) method,^{39,45} the concentric-cylinders (CC) method,^{40–44,46} the parallel-plates (PP) method,⁵⁰ and the transient hot-wire (THW) technique^{47–49,51,52} were used in the measurements of these data. In principle, the uncertainties associated with these experimental techniques decrease along this series of methods toward the THW method. However, most experimenters reported significantly lower error estimates than are accepted nowadays.

For the development of the zero-density contribution of their experimentally based correlation for methane Friend *et al.*³⁴ used as primary data the results of the THW measurements of Roder⁴⁹ and of the CC experiments of Le Neindre *et al.*⁴³ All the other available data were classified as secondary. Using a preliminary version of the residual contribution of their correlation, Friend *et al.* adjusted the lowest-density results of the isothermal measurements at atmospheric pressure of Le Neindre *et al.*⁴³ to zero density. For Roder's data⁴⁹ no such extrapolation was necessary as the tabulated values⁴⁹ were given in the limit of zero density. It should be noted that the effect of the initial density dependence of the thermal conductivity is in fact small and that the adjustment amounted to no more than 0.2%. Friend *et al.*³⁵ estimated the

uncertainty of their zero-density correlation to be $\pm 2.5\%$ between 130 and 625 K, the temperature range of the primary data selected.

Assael *et al.*³⁶ developed a theoretically based correlation for the zero-density thermal conductivity in the temperature range of 120–1000 K with uncertainties estimated to be $\pm 2\%$ between 300 and 500 K, $\pm 2.5\%$ at the lowest, and $\pm 4\%$ at the highest temperatures. These uncertainties originated from the analysis of thermal conductivity measurements, as well as from new theoretical results available at that time. Experimental THW values^{47–49,51} were chosen as primary data sets by Assael *et al.* They ascribed uncertainties of $\pm 0.5\%$ to these measurements, apart from those of Roder⁴⁹ ($\pm 2\%$). To avoid a limited temperature range, they also included less reliable values obtained with the HW technique^{39,45} [$\pm 3\%$ (Ref. 39) and $\pm 1\%$ (Ref. 45)] and the CC method⁴⁴ ($\pm 2.5\%$). They made use of the theoretical high-temperature limiting behavior of the ratio of the diffusion coefficient for internal energy, D_{int} , to the self-diffusion coefficient, D , in order to provide a reliable extrapolation of the experimental thermal conductivity data.

Uribe *et al.*^{37,38} used the THW data of Clifford *et al.*,⁴⁷ Assael and Wakeham,⁴⁸ and Millat *et al.*⁵¹ as primary data sets for their correlation for methane. Their correlation scheme combines kinetic theory with an extended principle of corresponding states to calculate the thermal conductivity of a series of polyatomic gases at zero density. This scheme offers somewhat more predictive power than the correlation of Assael *et al.*,³⁶ which fits each gas individually. Similarly to the procedure of Assael *et al.*,³⁶ kinetic theory has been used by Uribe *et al.*^{37,38} to underpin the extrapolation to high temperatures. The analysis resulted in a correlation depending on the high-temperature limiting value of the collision number for rotational relaxation $\zeta_{\text{rot}}^{\infty}$ and on a crossover temperature T_{cross} for switching between two relations for the temperature function of the diffusion coefficient for rotational energy D_{rot} . Both parameters have been treated as adjustable and have been fixed individually for each gas. Uribe *et al.*³⁸ estimated the uncertainty of their correlation for λ to be $\pm 1.5\%$ in the temperature range of 300–500 K, deteriorating to $\pm 3\%$ at lower and higher temperatures.

In addition to the experimental data considered by the authors of these three correlations, we included in our comparison further experimental values.^{40,50,52} In particular, the PP values of Hemminger⁵⁰ should be very useful, since he performed careful corrections for the contamination by air desorbed from the measuring instrument.

Figure 2 illustrates very good overall agreement between the calculated and measured values. In particular, the calculated values agree with the correlation of Friend *et al.*³⁴ within its estimated uncertainty over the whole of the temperature range. Similar agreement is observed with the correlations of Assael *et al.*³⁶ and of Uribe *et al.*,^{37,38} everywhere except in the temperature range of approximately 350–550 K, where the deviations are just outside the claimed uncertainty of the correlations. The direct comparison with the experimental data also illustrates very good agreement. In most cases,^{39–49,52} the agreement is within the experimental uncertainty ascribed to the data by correlation developers.

More importantly the calculated values are in excellent agreement (-0.5% to -1.0%) with the experimental point of Assael and Wakeham⁴⁸ at 308 K as well as the data of Hemminger.⁵⁰ Based partly on the agreement of Hemminger's measurements on nitrogen, which have already been discussed by Bich *et al.*⁵ (see Fig. 6 in that reference), both these data sets of Hemminger are considered to be of very high quality.

The only data set which is in disagreement with the calculated values is the transient HW data of Millat *et al.*,⁵¹ which up to now have been assumed to constitute excellent primary data. The experimental datum at 425 K is about 4% higher than both the correlation of Friend *et al.*³⁴ and the present calculated value. A detailed inspection of Fig. 2 also shows that the temperature dependence of the data of Millat *et al.*⁵¹ disagrees with that of most other data, as well as with that of our calculated values. It appears that the measurements of Millat *et al.*⁵¹ at higher temperatures are erroneous and that, at most, only the measurement at 309 K can be considered as a primary datum.

The experimental data of Millat *et al.*⁵¹ had a strong impact on the development of the correlations of Assael *et al.*³⁶ and Uribe *et al.*,^{37,38} as both correlations considered these as primary data. Hence both correlations mimic, up to about 400 K, the temperature dependence of these data. Not surprisingly, the inclusion of this data set in the analysis leads to a less accurate extrapolation to higher temperature for both correlations. Based on the good agreement of the calculated values with all the other high-temperature data and on the theoretical background of the calculated values of the present paper, we consider that the values of the thermal conductivity obtained in this work at high temperatures are more reliable than the values obtained from the correlations of Assael *et al.*³⁶ and of Uribe *et al.*^{37,38}

Concerning the low-temperature region, although there also exist differences between the three correlations and our calculated values, these differences fall within the uncertainty claimed for all the correlations. Because Friend *et al.*³⁴ and Assael *et al.*³⁶ selected different experimental values as primary data, their correlations differ quite significantly at low temperatures. Based on the agreement of our calculated values with the experimental data and on similar agreement observed for viscosity, we consider that the present calculations provide the best estimate of the thermal conductivity of methane at temperatures lower than 200 K. Taking account of the comparison with the available data, especially around room temperature, and the accuracy of the intermolecular potential used, we estimate the accuracy of the computed values to be of the order of $\pm(1-1.5)\%$ in the complete temperature range between 80 and 1500 K. Values of the calculated thermal conductivity are included in the information deposited with the Electronic Physics Auxiliary Publication Service.³²

B. Thermomagnetic effects

Seven independent measurements of thermomagnetic effects in methane^{53–59} have been reported. Following the analysis of the data by the authors and our own analysis, we

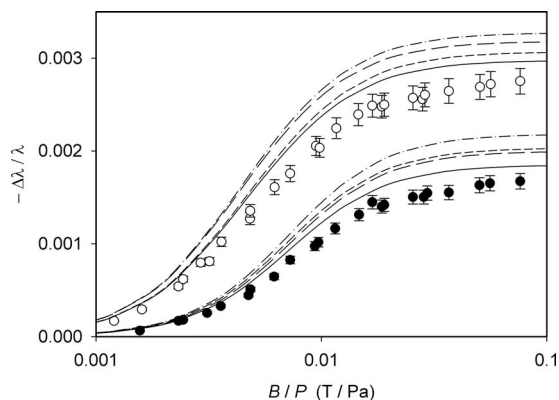


FIG. 3. Comparison of the measurements of Hermans *et al.* (Ref. 58) of the thermomagnetic effect at 300 K with the present calculations. Experimental values: (○) $-\Delta\lambda^\perp/\lambda$; (●) $-\Delta\lambda^\parallel/\lambda$. Calculations: (---) \mathbf{W}_{jj} polarization, SA only; (-.-.-) \mathbf{W}_{jj} polarization, full calculation; (—) $\mathbf{W}_{jj}+\mathbf{W}_j$ polarizations, both using the SA; (—) \mathbf{W}_{jj} polarization, full calculation, combined with \mathbf{W}_j polarization, SA. The error bars shown correspond to the estimated experimental uncertainty (Ref. 58) of $\pm 5\%$.

classified the four more recent measurements^{53,57–59} as primary. All the measurements were made either in single or double cylindrical cells placed between two parallel plates that could be heated. Hermans *et al.*⁵⁷ measured the transverse thermomagnetic coefficient at approximately 85 K for (B/P) values up to 0.076 T/Pa ($\equiv 100$ kOe/torr) with an accuracy of 15%.⁵⁹ Shortly afterwards Hermans *et al.*⁵⁸ carried out measurements of the two longitudinal coefficients, $\Delta\lambda^\perp/\lambda$ and $\Delta\lambda^\parallel/\lambda$, at 300 K at (B/P) values of up to 0.076 T/Pa ($\equiv 100$ kOe/torr), with an estimated accuracy of 3%–5%. As both longitudinal coefficients have been measured in the same apparatus, the authors assumed that cancellation of systematic errors will make the ratio of the two coefficients accurate to 2%. Both longitudinal coefficients were further measured by Heemskerck *et al.*⁵⁹ at about 85 K at (B/P) values of up to 0.16 T/Pa ($\equiv 220$ kOe/torr) with an estimated accuracy of 5%. Subsequently, Heemskerck *et al.*⁵³ measured the coefficients $\Delta\lambda^\perp/\lambda$ and $\Delta\lambda^\parallel/\lambda$ at 150 and 200 K at (B/P) values of up to 0.06 T/Pa ($\equiv 80$ kOe/torr), with uncertainties estimated at 2% for the ratio of these coefficients and 3% for their values at saturation, i.e., at high B/P values.

For the thermomagnetic coefficients $\Delta\lambda^\perp/\lambda$ and $\Delta\lambda^\parallel/\lambda$ Fig. 3 shows the comparison between the calculated values and the available experimental data (read from the published figures) at 300 K.⁵⁸ Although it is clear that the dominant contribution comes from \mathbf{W}_{jj} polarization, a single polarization cannot represent the experimental data within their uncertainties. Hence, to provide an improved description of the thermomagnetic effect, we tested the two approaches discussed in Sec. II B. As illustrated in Fig. 3, using the full \mathbf{W}_{jj} expression without making the SA will lower the values of the two coefficients and improve the agreement with the experiments. At saturation the full description lies about 7% below the SA values.

Taking a different approach and retaining the SA but invoking a second polarization, \mathbf{W}_j , results also shown on the figure, again leads to better agreement with experiment, yielding a lowering of the saturation values, $(\Delta\lambda^\perp/\lambda)_{\text{sat}}$ and

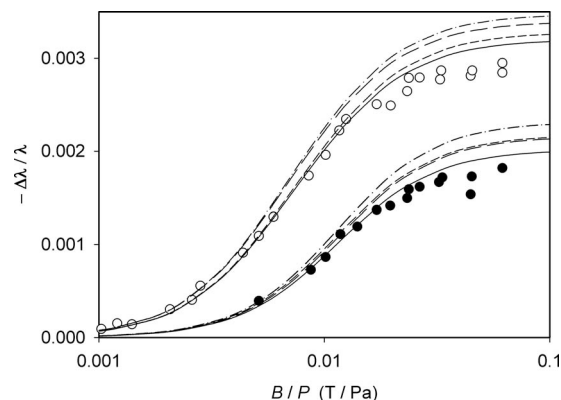


FIG. 4. Comparison of the measurements of Heemskerck *et al.* (Ref. 53) of the thermomagnetic effect at 200 K with the present calculations. Symbols and lines are the same as in Fig. 3.

$(\Delta\lambda^\parallel/\lambda)_{\text{sat}}$, by 3% and 9%, respectively, from the SA values with just the \mathbf{W}_{jj} polarization. There is currently no theory which provides a full treatment, without the SA, in terms of two polarizations. Considering that the effects of both improvements are small, less than 10%, we estimated their overall effect by adding the two effects. The overall longitudinal thermomagnetic coefficients estimated in this way are consistent with the experimental data, the slight overestimate of the experimental data being just outside the quoted uncertainties.

Figure 4 shows a similar comparison between the calculated and measured values of the longitudinal thermomagnetic coefficients at 200 K.⁵³ Based on the entries in Table III of this reference, we have taken the measured values from Fig. 7, as the caption appears to have been interchanged with that for Fig. 6. While the contributions due to the full treatment of \mathbf{W}_{jj} , or the addition of the \mathbf{W}_j polarization, decrease slightly with temperature, both these corrections are still necessary in order to get good agreement with experiment. The values of the $\Delta\lambda^\perp/\lambda$ and $\Delta\lambda^\parallel/\lambda$ coefficients calculated by combining the two effects are in very good agreement with the experimental data.

Finally, Fig. 5 shows the comparison of the calculated values of all three thermomagnetic coefficients, $\Delta\lambda^\perp/\lambda$,

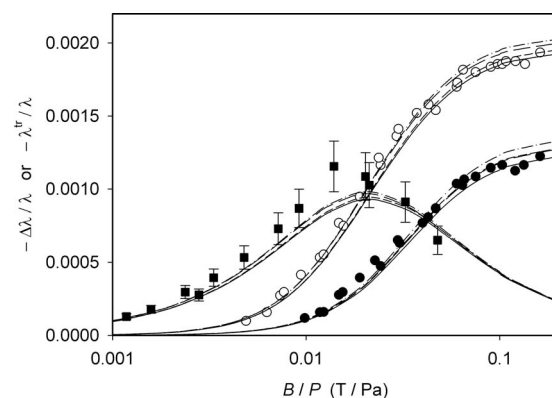


FIG. 5. Comparison of the measurements of Heemskerck *et al.* (Ref. 59) and of Hermans *et al.* (Ref. 57) of the thermomagnetic effect at about 85 K with the present calculations. Experimental values: (○) $-\Delta\lambda^\perp/\lambda$; (●) $-\Delta\lambda^\parallel/\lambda$; (■) $-\lambda^{\text{tr}}/\lambda$. Lines are the same as in Fig. 3. The error bars shown for $\lambda^{\text{tr}}/\lambda$ correspond to the estimated experimental uncertainty of $\pm 15\%$.

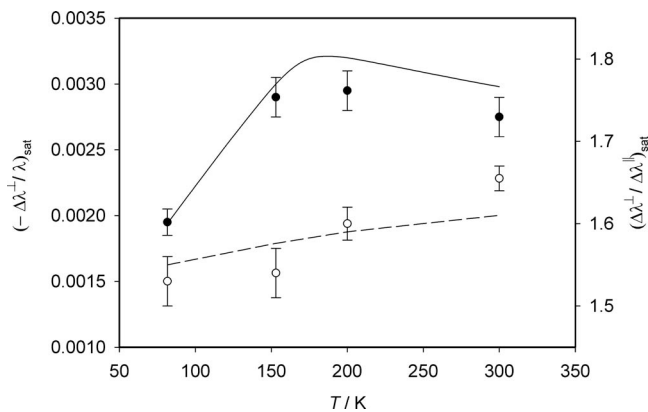


FIG. 6. Comparison between thermomagnetic coefficients at saturation obtained from the experimental analysis (Ref. 53) with the present full calculations as described in the text. Left ordinate: $(-\Delta\lambda^\perp/\lambda)_{\text{sat}}$; (●) experimental values; (—) calculations. Right ordinate: $(\Delta\lambda^\perp/\Delta\lambda^\parallel)_{\text{sat}}$; (○) experimental values; (---) calculations.

$\Delta\lambda^\parallel/\lambda$, and $\lambda^{\text{tr}}/\lambda$, with the available experimental data at about 85 K.^{57,59} Note that these data are available at a wider range of (B/P) values than those at the other temperatures. The agreement with the experimental data is excellent and not only are the two longitudinal coefficients reproduced within the experimental error, but so also is the transverse coefficient. The good agreement observed at such a low temperature is encouraging for the use of a classical-trajectory calculation.

Heemskerck *et al.*⁵³ analyzed the data^{53,58,59} on the thermomagnetic coefficients $\Delta\lambda^\perp/\lambda$ and $\Delta\lambda^\parallel/\lambda$ of methane to draw some conclusions about the variation with temperature of a number of parameters and cross sections. We will not carry out the comparison at the level of cross sections, as these were unduly influenced by the analysis of the experimental data based only on the dominant polarization $\mathbf{W}_{\mathbf{j}\mathbf{j}}$ in the SA. However it is useful to compare with quantities that could be extracted more directly from the experimental data.

One such quantity is the saturation value of the longitudinal thermomagnetic coefficients. Although Heemskerck *et al.*⁵³ obtained these quantities by extrapolating the experimental data using equations based on the dominant polarization, $\mathbf{W}_{\mathbf{j}\mathbf{j}}$, and the SA, the extent of the data is such that the extrapolation was carried out in the region where the sensitivity to these approximations is small.

Figure 6 shows the comparison between the best calculated values of the perpendicular thermomagnetic coefficient at saturation, $(\Delta\lambda^\perp/\lambda)_{\text{sat}}$, and the values obtained from the experimental analysis. The agreement between the calculated and the measured values⁵³ decreases somewhat with increasing temperature. At the lowest temperature of the measurements (at about 85 K) the calculated value of 1.94×10^{-3} is well within the experimental uncertainty of the quoted value, $(1.95 \pm 0.1) \times 10^{-3}$, while at the highest temperature, 300 K, the calculated value of 2.98×10^{-3} slightly overestimates the quoted value of $(2.75 \pm 0.1) \times 10^{-3}$. The position $(B/P)_{1/2}^\perp$, that is the (B/P) value for which the $(\Delta\lambda^\perp/\lambda)$ curve reaches half the saturation value, not shown in Fig. 6, is also in very good agreement at low temperature: 19.1 mT/Pa compared with the quoted value of 19.8 ± 1.0 mT/Pa. At 300 K the

calculated value of 4.67 mT/Pa underestimates the quoted value of 5.1 ± 0.2 mT/Pa. This is not surprising considering that at 300 K the SA description based on a single $\mathbf{W}_{\mathbf{j}\mathbf{j}}$ polarization is more in error and the value of $(B/P)_{1/2}^\perp$ is sensitive to the shape of the function used for its determination.

Heemskerck *et al.*⁵³ also quoted a value of $(\Delta\lambda^\perp/\Delta\lambda^\parallel)_{\text{sat}}$ as a function of temperature. If only the single polarization $\mathbf{W}_{\mathbf{j}\mathbf{j}}$ is included, this ratio, in the SA, is independent of temperature and equal to 1.5. Our results indicate that, using the full $\mathbf{W}_{\mathbf{j}\mathbf{j}}$ expression, the value of this ratio changes only slightly, from 1.50 to 1.51, the value being nearly independent of temperature. However, if one includes the second polarization, $\mathbf{W}_{\mathbf{j}}$, in a spherical-approximation description, our calculations indicate a stronger temperature variation: from 1.54 at 80 K to 1.59 at 300 K and 1.7 at 1500 K. Hence, as noted by Hermans *et al.*,⁵⁸ the ratio $(\Delta\lambda^\perp/\Delta\lambda^\parallel)_{\text{sat}}$ is rather useful as its deviation from 1.5 primarily shows the influence of additional polarizations. Figure 6 illustrates the comparison between the calculated values of this ratio and the values obtained from the experimental analysis.⁵³ The measured values are reproduced to within $\pm 3\%$, which is just outside their estimated uncertainty.

C. Volume viscosity

Before the comparison with experiment we consider the magnitude and the temperature dependence of the higher-order corrections to the volume viscosity. The second-order correction is below 2% at 80 K, increasing to about 10% at room temperature and rising to 18% at 1500 K. The third-order result differs from the second-order result by less than 0.2% at temperatures up to 1500 K. The second-order correction is larger than those found for carbon monoxide⁴ and carbon dioxide⁷ but smaller than that found for nitrogen.²

Sound-absorption and, in some cases, sound dispersion, measurements in methane have been performed by Kelly⁶⁰ at 314 K, Holmes *et al.*⁶¹ at 303 K, Hill and Winter⁶² at 298, 573, 773, and 1073 K, Kistemaker *et al.*⁶³ at 308.3 K, and Prangma *et al.*²³ at 77.1, 180, 260, and 293 K. Of these, all except Prangma *et al.*²³ analyzed their results in terms of a relaxation time. We have converted these relaxation time values to volume viscosity values using Eq. (12). Figure 7 shows the comparison between our theoretical results and the measurements. The inset enlarges the region around room temperature. If an experimental uncertainty has been quoted we have shown it in the figure. For the measurement of Kelly⁶⁰ we have taken the uncertainty as the difference (18%) between values he obtained using the sound-absorption and the sound dispersion methods of analyzing his data.

The lowest temperature measurements, those at 77 and 180 K, uncertainty of $\pm 10\%$, exceed the calculated values by about 55% and 25%, respectively. For the measurements^{23,60-62} around room temperature, 293–314 K, our result is consistent with that of Prangma *et al.*²³ at 293 K but about 20% below the other measurements (derived from relaxation times), although the uncertainties of two of these are comparable with the difference.

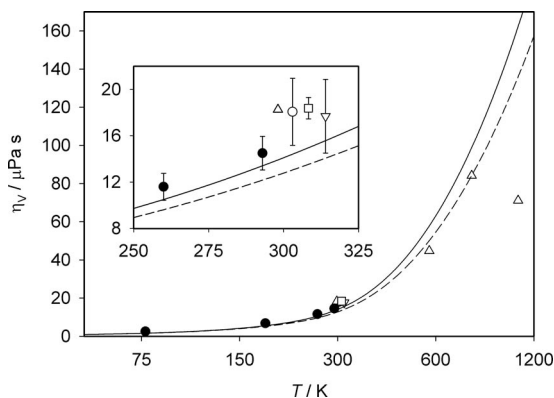


FIG. 7. Comparison of experimentally based values for the volume viscosity with the present calculations. Values inferred from rotational relaxation times: (∇) Kelly (Ref. 60); (\circ) Holmes *et al.* (Ref. 61); (\triangle) Hill and Winter (Ref. 62); (\square) Kistemaker *et al.* (Ref. 63). Experimental volume viscosity data: (\bullet) Prangma *et al.* (Ref. 23). Calculations: (---) first-order theory; (—) third-order theory.

While the high-temperature, 773 K, result of Hill and Winter⁶² is within 20% of the calculated value, at 1073 K the calculated value is more than twice that inferred from the measured relaxation time. We note that the vibrational relaxation time inferred by Hill and Winter⁶² at 298 K, 1.86 μ s, is almost double that measured more recently by Trusler and Zarari,⁶⁴ 0.997 \pm 0.006 μ s at 300 K.

Theory is generally consistent with the measurements, particularly when it is recalled²³ that a small error in the primary quantity measured, the sound-absorption coefficient, causes a relatively large error in derived quantities such as η_v . Examining the temperature dependence of the data of Hill and Winter⁶² in the whole of the measured range (298–1073 K) one comes to the conclusion that the accuracy of the highest temperature value may be relatively low. In this case the separation of the rotational and vibrational contributions to the measurements may need further refinement.

More recently, measurements of relaxation in free jets have been used by Abad *et al.*⁶⁵ to infer a value of the rotational relaxation cross section, $\mathfrak{S}(0001)$. Because of the nature of these experiments the authors were able to conclude only that the expression $\mathfrak{S}(0001)(T) = 5.0 \text{ \AA}^2(298 \text{ K}/T)^{0.9}$ was consistent with their measurements over the temperature range of 15–100 K. From their Fig. 9, indicating the range of cross section values compatible with their measurements, we have inferred an uncertainty of between 25% and 35%. We note that this result is consistent with that of Prangma *et al.*²³ at 77.1 K, discussed above. At this temperature the third-order result for the volume viscosity differs from the first-order result by about 3%. At a temperature of 100 K the calculated value of $\mathfrak{S}(0001)$ is about 50% larger than the value of Abad *et al.*,⁶⁵ so outside their estimated uncertainty of about 35%.

Strekalov⁶⁶ analyzed Q -branch Raman line-shape data at 295 K to infer a value for $\mathfrak{S}(0001)$ of 5.4 Å^2 , compared to the calculated value of 7.2 Å^2 . As Strekalov⁶⁶ did not provide any estimate of the uncertainty in his value, necessarily obtained via an elaborate analysis, it is difficult to assess the significance of the apparent discrepancy with theory.

In He–N₂ collisions¹⁴ quantal effects for $\mathfrak{S}(0001)$ are

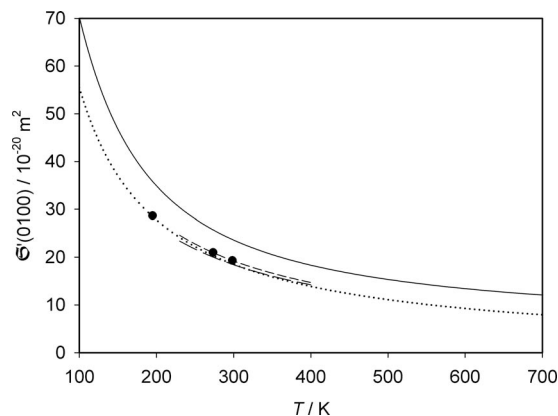


FIG. 8. Comparison of values of the cross section $\mathfrak{S}'(0100)$ inferred from nuclear-spin relaxation measurements with the present calculations. Experimental values: (·····) Bloom *et al.* (Ref. 26) and Lalita and Bloom (Ref. 67), using ^1H ; (\bullet) Gerritsma *et al.* (Ref. 70), using ^1H ; (—) Jameson *et al.* (Ref. 28), using ^1H ; (---) Jameson *et al.* (Ref. 28), using ^{13}C . This work: (—).

less than 4% for temperatures above 77 K. However, while the rotor constant for nitrogen is 2.01 cm^{-1} , that for methane is 5.4 cm^{-1} and, because of the nuclear-spin symmetry, methane has more complex selection rules for transitions between rotational energy levels. Hence quantal effects may be significant at low temperatures.

D. Nuclear-spin relaxation

Bloom *et al.*²⁶ measured the relaxation of the proton spins in methane for temperatures between 100 and 300 K. These measurements were complemented by Lalita and Bloom,⁶⁷ who covered the temperature range from room temperature to 700 K. They noted that their expression for the cross section as a function of temperature was consistent with earlier measurements at or below room temperature.^{25,26,68,69} Other measurements at temperatures of 194.75, 273.15, and 298.15 K were reported at about the same time by Gerritsma *et al.*⁷⁰ For these we have employed the values at the lowest number density for which results are reported. Jameson *et al.*²⁸ repeated the measurements of proton spin relaxation and extended these measurements to the relaxation of the ^{13}C nuclear spin in $^{13}\text{CH}_4$ for temperatures between 230 and 400 K. The analogous spin-rotation relaxation mechanism applies. The relative error in the relaxation time was estimated²⁸ to be typically less than 1% and the uncertainty in the inferred cross section values was about 2%. The proton spin relaxation measurements appear consistent, within experimental error, with a single relaxation time.^{26,28,29}

Calculated values of $\mathfrak{S}'(0100)$ are compared in Fig. 8 with the values inferred from the measurements.^{26,28,67,70} Agreement among the measured values is good. The theoretical results are consistently higher than the experimental values based on proton relaxation by about 25% at 100 K, 27% at room temperature, and 50% at 700 K. For the temperatures of 230–400 K for which ^{13}C results are also available, the difference from the calculated values is about 4% smaller. It should be realized that the analysis of the ^{13}C nuclear-spin relaxation does not require such an elaborate

discussion²⁹ as that for the four proton spins in $^{12}\text{CH}_4$. This quite independent measurement using ^{13}C nuclear-spin relaxation gives strong confirmation of the accuracy of the series of measurements of $\mathcal{S}'(0100)$ using $^{12}\text{CH}_4$.

For carbon dioxide the calculated value⁸ of the $\mathcal{S}'(0100)$ cross section using three different potential surfaces generally underestimated the value obtained by Jameson *et al.*⁷¹ from NMR relaxation measurements. In carbon monoxide the calculated value⁴ overestimated the corresponding measured value. In nitrogen the calculated values⁷² were broadly consistent with the measurements for both the $\mathcal{S}'(0100)$ and $\mathcal{S}'(0200)$ cross sections. Clearly NMR observations are among the most difficult to reproduce accurately.

IV. SUMMARY AND CONCLUSIONS

We have calculated the values of the thermal conductivity, thermomagnetic effects, thermal transpiration, volume viscosity, and nuclear-spin relaxation by means of the classical-trajectory method using a full anisotropic rigid-rotor methane-methane potential energy hypersurface.

For thermal conductivity very good agreement is obtained between the calculated and measured values. In most cases the agreement with the primary experimental data is within the uncertainty ascribed to the data by the correlation developers. The comparison with the most accurate experimental data by Assael and Wakeham⁴⁸ and Hemminger⁵⁰ shows relatively constant deviations of -0.5% to -1.0% in the temperature range of 310–480 K indicating that, analogous to viscosity, a correction at room temperature to the calculated values of the thermal conductivity of the order of -0.5% could be appropriate.

The influence of the vibrational degrees of freedom and the second-order contribution were established to be small, less than 0.2% and 0.5%, respectively, in thermal conductivity. The Thijssse approximation, Eq. (3), gave very good estimates, in line with the findings for other molecules studied. Overall, the theoretical background of the calculated thermal conductivity values is well founded, and their uncertainty is estimated to be of the order of $\pm(1-1.5)\%$. These calculations are expected to be more reliable than the correlations currently available in the open literature, as well as most of the measurements in the complete temperature range between 80 and 1500 K. While the temperature dependence of the calculated values at high temperatures should be very reliable, quantal effects cannot be excluded at low temperatures. Good agreement is also obtained with the values inferred from thermal transpiration experiments for the translational Eucken factor f_{tr} .

We have made use of our calculation of the thermomagnetic effect to establish the influence of a second polarization and of the full treatment on the thermomagnetic coefficients. Although the dominant contribution comes from the \mathbf{W}_{jj} polarization in the SA, the influence of the second polarization \mathbf{W}_j and of the full \mathbf{W}_{jj} description should not be ignored. At saturation the combined effect of the latter two contributions is of the order of 10%–15% at room temperature.

Measurements of the thermomagnetic effect are in very good agreement with the calculated values over the whole temperature range (85–300 K) examined. It is especially encouraging that all three thermomagnetic coefficients at 85 K are reproduced within their experimental accuracy as this gives further support for the use of classical-trajectory calculations at such low temperatures. Further good agreement was observed with the measured values of the longitudinal thermomagnetic coefficients at saturation and also with the position of the half-saturation value. The agreement at room temperature was just outside the claimed uncertainty.

The experimental data for volume viscosity are characterized by much larger uncertainty than for other properties studied. The claimed uncertainty of the individual data sets, more often than not, is much less than the differences obtained between what should be comparable data sets from independent observations. Furthermore, most of the available values have been inferred from the measurements of the relaxation times by means of an approximate relationship. Nevertheless, the majority of the measurements around room temperature yielding the volume viscosity are consistent with the calculated values. At high and low temperatures our calculated values underestimate and overestimate, respectively, the measured data by approximately 20%–100%. It is possible that at low-temperatures quantal effects might influence the volume viscosity more than they do thermal conductivity and thermomagnetic effects. However, at high temperatures we believe that the claimed accuracy of the experimental values may be rather optimistic and that further refinement of the separation of the rotational and vibrational contributions should be undertaken.

A number of available nuclear-spin relaxation data sets from different laboratories are mutually consistent within a few percent. However, the calculated values of nuclear-spin relaxation, sensitive primarily to the anisotropy, consistently exceed the measurements by between approximately 25% and 50% in the temperature range of 100–700 K. For other molecules studied the nuclear-spin relaxation data were also difficult to reconcile with the calculated values. The reason for this disagreement is unclear at this stage. However, the theory is not as well tested as that for the thermal conductivity and the thermomagnetic properties.

Measurements are also available for the volume viscosity^{23,61,73} and the nuclear-spin relaxation⁷⁴ of tetradeteromethane. These will be discussed in a separate publication.

ACKNOWLEDGMENTS

This work was financially supported by the German Research Foundation (Deutsche Forschungsgemeinschaft), Grant No. VO 499/14-1.

¹E. L. Heck and A. S. Dickinson, *Mol. Phys.* **81**, 1325 (1994).

²E. L. Heck, A. S. Dickinson, and V. Vesovic, *Mol. Phys.* **83**, 907 (1994).

³E. L. Heck and A. S. Dickinson, *Physica A* **217**, 107 (1995).

⁴E. L. Heck and A. S. Dickinson, *Physica A* **218**, 305 (1995).

⁵E. Bich, S. Bock, and E. Vogel, *Physica A* **311**, 59 (2002).

⁶S. Bock, E. Bich, E. Vogel, A. S. Dickinson, and V. Vesovic, *J. Chem. Phys.* **117**, 2151 (2002).

⁷S. Bock, E. Bich, E. Vogel, A. S. Dickinson, and V. Vesovic, *J. Chem.*

- Phys.* **120**, 7987 (2004).
- ⁸ S. Bock, E. Bich, E. Vogel, A. S. Dickinson, and V. Vesovic, *J. Chem. Phys.* **121**, 4117 (2004).
- ⁹ M. R. Swain, G. Vasisht, and G. Tinetti, *Nature (London)* **452**, 329 (2008).
- ¹⁰ R. Hellmann, E. Bich, E. Vogel, A. S. Dickinson, and V. Vesovic, *J. Chem. Phys.* **129**, 064302 (2008).
- ¹¹ F. R. W. McCourt, J. J. M. Beenakker, W. E. Köhler, and I. Kučšer, *Nonequilibrium Phenomena in Polyatomic Gases* (Oxford Science, Oxford, 1990), Vol. 1.
- ¹² R. Hellmann, E. Bich, and E. Vogel, *J. Chem. Phys.* **128**, 214303 (2008).
- ¹³ F. R. W. McCourt, V. Vesovic, W. A. Wakeham, A. S. Dickinson, and M. Mustafa, *Mol. Phys.* **72**, 1347 (1991).
- ¹⁴ V. Vesovic, W. A. Wakeham, A. S. Dickinson, F. R. W. McCourt, and M. Thachuk, *Mol. Phys.* **84**, 553 (1995).
- ¹⁵ J. H. Ferziger and H. G. Kaper, *The Mathematical Theory of Transport Processes in Gases* (North Holland, Amsterdam, 1972).
- ¹⁶ Y. Kagan and A. M. Afanasev, *Sov. Phys. JETP* **14**, 1096 (1962).
- ¹⁷ L. A. Viehland, E. A. Mason, and S. I. Sandler, *J. Chem. Phys.* **68**, 5277 (1978).
- ¹⁸ G. C. Maitland, M. Mustafa, and W. A. Wakeham, *J. Chem. Soc., Faraday Trans. 2* **79**, 1425 (1983).
- ¹⁹ G. C. Maitland, M. Rigby, E. B. Smith, and W. A. Wakeham, *Intermolecular Forces: Their Origin and Determination* (Clarendon, Oxford, 1987).
- ²⁰ B. J. Thijsse, W. A. P. Denissen, L. J. F. Hermans, H. F. P. Knaap, and J. J. M. Beenakker, *Physica A* **97**, 467 (1979).
- ²¹ A. Tip, *Physica (Amsterdam)* **37**, 82 (1967).
- ²² G. W. 't Hooft, E. Mazur, J. M. Bienfait, L. J. F. Hermans, H. F. P. Knaap, and J. J. M. Beenakker, *Physica A* **98**, 41 (1979).
- ²³ G. J. Prangma, A. H. Alberga, and J. J. M. Beenakker, *Physica (Amsterdam)* **64**, 278 (1973).
- ²⁴ J. D. Lambert, *Vibrational and Rotational Relaxation in Gases* (Clarendon, Oxford, 1977).
- ²⁵ C. S. Johnson, Jr. and J. S. Waugh, *J. Chem. Phys.* **35**, 2020 (1961).
- ²⁶ M. Bloom, F. Bridges, and W. N. Hardy, *Can. J. Phys.* **45**, 3533 (1967).
- ²⁷ P. H. Oosting and N. J. Trappeniers, *Physica* **51**, 418 (1971).
- ²⁸ C. J. Jameson, A. K. Jameson, N. C. Smith, J. K. Hwang, and T. Zia, *J. Phys. Chem.* **95**, 1092 (1991).
- ²⁹ P. A. Beckmann, M. Bloom, and I. Ozier, *Can. J. Phys.* **54**, 1712 (1976).
- ³⁰ E. L. Heck and A. S. Dickinson, *Comput. Phys. Commun.* **95**, 190 (1996).
- ³¹ R. Hellmann, E. Bich, and A. S. Dickinson, *Comput. Phys. Commun.* (in preparation).
- ³² See EPAPS Document No. E-JCPSA6-130-049912 for electronic files that contain these tables. For more information on EPAPS, see <http://www.aip.org/pubserve/epaps.html>.
- ³³ J. Millat, A. Plantikow, D. Mathes, and H. Nimz, *Z. Phys. Chem. (Leipzig)* **269**, 865 (1988).
- ³⁴ D. G. Friend, J. F. Ely, and H. Ingham, *J. Phys. Chem. Ref. Data* **18**, 583 (1989).
- ³⁵ D. G. Friend, J. F. Ely, and H. Ingham, National Institute of Standards and Technology Technical Note No. 1325, 1989.
- ³⁶ M. J. Assael, J. Millat, V. Vesovic, and W. A. Wakeham, *J. Phys. Chem. Ref. Data* **19**, 1137 (1990).
- ³⁷ F. J. Uribe, E. A. Mason, and J. Kestin, *Physica A* **156**, 467 (1989).
- ³⁸ F. J. Uribe, E. A. Mason, and J. Kestin, *J. Phys. Chem. Ref. Data* **19**, 1123 (1990).
- ³⁹ H. L. Johnston and E. R. Grilly, *J. Chem. Phys.* **14**, 233 (1946).
- ⁴⁰ I. F. Golubev, *Teploenergetika* **10**, 78 (1963).
- ⁴¹ D. Misić and G. Thodos, *Physica (Amsterdam)* **32**, 885 (1966).
- ⁴² V. P. Sokolova and I. F. Golubev, *Teploenergetika* **14**, 91 (1967).
- ⁴³ B. Le Neindre, R. Tufeu, P. Bury, P. Johannin, and B. Vodar, *Proceedings of the Eighth Conference on Thermal Conductivity*, 1968, edited by C. Y. Ho and R. E. Taylor (Plenum, New York, 1969), p. 229.
- ⁴⁴ R. Tufeu, B. Le Neindre, and P. Bury, *Physica (Amsterdam)* **44**, 81 (1969).
- ⁴⁵ A. A. Clifford, E. Dickinson, and P. Gray, *J. Chem. Soc., Faraday Trans. 1* **72**, 1997 (1976).
- ⁴⁶ Y. Tanaka, M. Noguchi, H. Kubota, and T. Makita, *J. Chem. Eng. Jpn.* **12**, 171 (1979).
- ⁴⁷ A. A. Clifford, J. Kestin, and W. A. Wakeham, *Physica A* **97**, 287 (1979).
- ⁴⁸ M. J. Assael and W. A. Wakeham, *J. Chem. Soc., Faraday Trans. 1* **77**, 697 (1981).
- ⁴⁹ H. M. Roder, *Int. J. Thermophys.* **6**, 119 (1985).
- ⁵⁰ W. Hemminger, *Int. J. Thermophys.* **8**, 317 (1987).
- ⁵¹ J. Millat, M. Ross, W. A. Wakeham, and M. Zalaf, *Physica A* **148**, 124 (1988).
- ⁵² J. Pátek and J. Klomfar, *Fluid Phase Equilib.* **198**, 147 (2002).
- ⁵³ J. P. J. Heemskerk, F. G. Van Kuik, H. F. P. Knaap, and J. J. M. Beenakker, *Physica (Amsterdam)* **71**, 484 (1974).
- ⁵⁴ L. J. F. Hermans, P. H. Fortuin, H. F. P. Knaap, and J. J. M. Beenakker, *Phys. Lett.* **25A**, 81 (1967).
- ⁵⁵ J. Korving, W. I. Honeywell, T. K. Bose, and J. J. M. Beenakker, *Physica (Amsterdam)* **36**, 198 (1967).
- ⁵⁶ L. J. F. Hermans, J. M. Koks, H. F. P. Knaap, and J. J. M. Beenakker, *Phys. Lett.* **30A**, 139 (1969).
- ⁵⁷ L. J. F. Hermans, A. Schutte, H. F. P. Knaap, and J. J. M. Beenakker, *Physica (Amsterdam)* **46**, 491 (1970).
- ⁵⁸ L. J. F. Hermans, J. M. Koks, A. F. Hengeveld, and H. F. P. Knaap, *Physica (Amsterdam)* **50**, 410 (1970).
- ⁵⁹ J. P. J. Heemskerk, L. J. F. Hermans, G. F. Bulting, and H. F. P. Knaap, *Physica (Amsterdam)* **57**, 381 (1972).
- ⁶⁰ B. T. Kelly, *J. Acoust. Soc. Am.* **29**, 1005 (1957).
- ⁶¹ R. Holmes, G. R. Jones, and N. Pusat, *Trans. Faraday Soc.* **60**, 1220 (1964).
- ⁶² G. L. Hill and T. G. Winter, *J. Chem. Phys.* **49**, 440 (1968).
- ⁶³ P. G. Kistemaker, M. M. Hanna, A. Tom, and A. E. de Vries, *Physica (Amsterdam)* **60**, 459 (1972).
- ⁶⁴ J. P. M. Trusler and M. Zarari, *J. Chem. Thermodyn.* **24**, 973 (1992).
- ⁶⁵ L. Abad, D. Bermejo, V. J. Herrero, J. Santos, and I. Tanarro, *J. Phys. Chem. A* **101**, 9276 (1997).
- ⁶⁶ M. L. Strekalov, *Mol. Phys.* **100**, 1049 (2002).
- ⁶⁷ K. Lalita and M. Bloom, *Chem. Phys. Lett.* **8**, 285 (1971).
- ⁶⁸ M. Bloom, M. Lipsicas, and B. H. Muller, *Can. J. Phys.* **39**, 1093 (1961).
- ⁶⁹ N. J. Trappeniers, C. J. Gerritsma, and P. H. Oosting, *Physica (Amsterdam)* **31**, 202 (1965).
- ⁷⁰ C. J. Gerritsma, P. H. Oosting, and N. J. Trappeniers, *Physica (Amsterdam)* **51**, 381 (1971).
- ⁷¹ C. J. Jameson, A. K. Jameson, N. C. Smith, and K. Jackowski, *J. Chem. Phys.* **86**, 2717 (1987).
- ⁷² D. Cappelletti, F. Pirani, F. Vecchiocattivi, E. L. Heck, and A. S. Dickinson, *Mol. Phys.* **93**, 485 (1998).
- ⁷³ P. G. Kistemaker, M. M. Hanna, and A. E. de Vries, *Physica (Amsterdam)* **78**, 457 (1974).
- ⁷⁴ M. A. ter Horst, C. J. Jameson, and A. K. Jameson, *Magn. Reson. Chem.* **44**, 241 (2006).